Eccentricity Fault Diagnosis based on Phase and Amplitude Features of Stray Flux in Permanent Magnet Synchronous Generators

Ilyas Aladag[1], Taner Goktas[2], *Senior Member*, *IEEE* and Muslum Arkan[3]

[1]Department of Electrical and Energy, Kadirli Vocational School, Osmaniye Korkut Ata University, Osmaniye, TR
ilyasaladag@osmaniye.edu.tr
[2] Department of Electrical and Electronics Engineering, Dokuz Eylul University, Izmir, TR
taner.goktas@deu.edu.tr
[3]Department of Electrical and Electronics Engineering, Inonu University, Malatya, TR
muslum.arkan@inonu.edu.tr

Abstract

Detecting, quantifying and discriminating between static (SE) and dynamic eccentricity (DE) in Permanent Magnet Synchronous Generators (PMSGs) is a significant challenge for conventional diagnostic methods. This paper presents a novel, non-invasive hybrid fault detection methodology using the external stray flux signal. The core of this method is a new indicator based on the differential phase shift between signals from a three-sensor array. This novel phase-based feature is combined with spectral sideband amplitude analysis for a comprehensive diagnosis. The Finite Element Method (FEM) analyses demonstrate that the differential phase shift is a highly sensitive metric for detecting both SE and DE. Its magnitude also directly correlates with SE fault severity. Fault type discrimination is subsequently achieved by analyzing the sideband amplitudes. The integration of this novel phase-based detection with amplitude-based discrimination establishes a unique fault detection fingerprint. This hybrid approach provides a reliable detection and discrimination of eccentricity faults.

1. Introduction

Permanent Magnet Synchronous Generators (PMSGs) are increasingly employed in critical applications such as renewable energy systems. These generators exhibit key attributes of high efficiency and superior power density. These characteristics position them as a preferred alternative to conventional induction machines [1, 2]. Despite these benefits, PMSGs remain susceptible to various mechanical and electrical faults. Such faults can compromise operational reliability and result in costly maintenance. Among these faults, eccentricity is particularly critical. This mechanical defect is defined as a misalignment between the rotor and stator axes [3]. This condition generates an unbalanced magnetic pull (UMP). The UMP increases machine vibration and accelerates the wear of mechanical components such as bearings [4]. The early and accurate detection of eccentricity is therefore critical. An undetected fault can progress in severity over time. This progression increases the risk of stator-rotor rub. Such contact may lead to catastrophic failure and forced system outages. The root causes of eccentricity include manufacturing imperfections and the gradual degradation of mechanical components such as bearings.

The literature presents numerous methods for detecting eccentricity faults in PMSGs. Online condition monitoring techniques are particularly prominent among these approaches. Motor Current Signature Analysis (MCSA) has emerged as one of the most widely established techniques due to its noninvasive nature and its capability to utilize existing current measurements available in motor drive systems. [5, 6]. However, MCSA has significant diagnostic limitations. The primary challenge is diagnostic ambiguity. For instance, distinct faults like rotor eccentricity, demagnetization, and load unbalance can all produce identical frequency components. This ambiguity makes it difficult to determine the root cause of a fault from the current spectrum alone [7]. The diagnostic challenge is compounded when multiple faults coexist. Their spectral signatures can interact. This interaction may amplify harmonics to create false positives or cancel them to create false negatives [8]. Finally, MCSA's effectiveness depends on the motor topology and winding configuration. Its performance also declines under non-stationary operating conditions [9].

Flux-based monitoring methods present a robust alternative for overcoming these diagnostic challenges. Flux is a physical quantity intrinsically related to the machine's magnetic symmetry. It is also less affected by the behavior of closed-loop current controllers [10]. These techniques are broadly categorized into two approaches: invasive air-gap measurement and non-invasive external stray flux analysis (SFA). Invasive methods require the integration of sensors, such as Hall-effect sensors or search coils, directly into the machine's air gap or stator slots [11]. This approach exhibits high sensitivity for detecting fault-related anomalies in the flux pattern. However, this implementation is often not feasible for existing machines as it requires generator disassembly. It also increases manufacturing complexity and cost. Consequently, monitoring the external stray flux has emerged as a promising non-invasive alternative [12]. Conventional external SFA methods primarily evaluate the amplitude characteristics of the measured flux [13, 14]. This typically involves tracking peak signal values or analyzing the signal envelope. However, such amplitude-based approaches are limited in their ability to accurately quantify fault severity and discriminate between fault types. A single-point measurement often lacks the sufficient diagnostic information required for a comprehensive analysis [15]. Consequently, more advanced stray flux-based methods employ a three-sensor array to construct a stray flux space vector, which provides enhanced diagnostic insight [16].

This study addresses the limitations of conventional MCSA and stray flux analysis techniques. It proposes a non-invasive detection method based solely on the analysis of the external stray flux signal. The core of this methodology is the hybrid analysis of two complementary features from this signal: a phase feature and an amplitude feature. The phase feature is the differential phase shift. It serves as the primary metric for fault detection and severity quantification. The amplitude feature is the magnitude of characteristic spectral sidebands. It is used for fault discrimination between SE and DE. The integration of these two distinct features provides a comprehensive and reliable detection of eccentricity faults.

2. Proposed Methodology: A Hybrid Stray Flux Analysis

2.1. Modeling of Permanent Magnet Synchronous Generator and Eccentricity Faults

A two-dimensional (2D) finite element method (FEM) model was developed in Ansys® Maxwell-2D software. This model analyzes the PMSG's behavior under healthy, static eccentricity (SE), and dynamic eccentricity (DE) conditions. A time-stepping transient solver is employed to capture key performance indicators. These indicators include magnetic field distribution, stator currents, and electromagnetic torque. The simulated PMSG has a 36-slots, 12-poles configuration and is rated at 400 W with a fundamental frequency of 170 Hz [17]. The FEM model includes the precise geometric dimensions of the stator and rotor cores, the shapes of the permanent magnets, and the nonlinear B-H characteristics of the ferromagnetic materials, which helps ensure high-fidelity simulation results.

As shown in Fig. 1, three sensing points (A, B, and C) are placed on the generator frame to capture the external stray flux. These sensors are positioned with a mechanical interval of 20°. For the simulated 12-pole machine (p = 6 pole pairs), this mechanical interval corresponds to a 120-degree electrical phase shift. In the transient simulation, the stray flux signals are sampled at 2.5 kHz for a duration of 5 seconds. This setup provides sufficient resolution for the subsequent spectral analysis.

To simulate fault conditions, two types of eccentricity have modeled. In SE, the rotor's axis of rotation has shifted away from the stator's geometric center. For DE, the rotor's geometric center has displaced relative to the axis of rotation, which remained fixed at the stator center. For both fault types, the severity has varied parametrically from 5% to 60% of the nominal air-gap length. All simulations have performed under full rated load conditions.

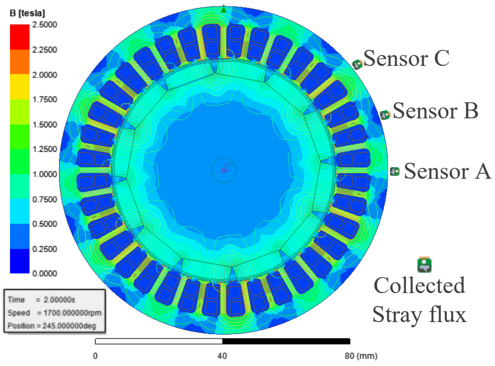

Fig.1. 2D FEM model of PMSG with the external stray flux sensors

2.2. Physical Principle of Eccentricity Signatures in Stray Flux

Rotor eccentricity faults introduce a geometric asymmetry that disrupts the uniformity of the air-gap length between the stator and rotor. The resulting structural change alters the magnetic permeance path and leads to distortion in the magnetic field generated by the permanent magnets. The external stray flux is functionally related to the main air-gap flux. Therefore, these internal magnetic distortions extend to the exterior of the machine frame. This extension produces measurable signatures suitable for diagnostic analysis.

The proposed hybrid approach first uses the differential phase shift to detect an eccentricity fault. Both SE and DE produce a significant differential phase shift. An SE fault creates a fixed spatial asymmetry in the air gap. This stationary distortion of the magnetic field causes the flux wave to reach each sensor at a different time. Similarly, a DE fault creates a rotating spatial asymmetry. This asymmetry also distorts the magnetic field at any given instant. This distortion leads to a measurable phase shift between the sensors.

Once a fault is detected via phase shift, sideband amplitude analysis is performed for differentiation. In a DE fault, the point of minimum air gap rotates with the rotor. This rotation causes a strong, time-varying modulation of the air-gap permeance. This periodic modulation is the primary source of high-amplitude spectral sidebands. However, the stationary asymmetry of an SE fault does not create a significant time-varying modulation. An SE fault therefore generates the same sideband harmonics but with substantially lower amplitudes.

The proposed hybrid method analyzes two distinct features of the external stray flux. The first feature is the differential phase shift, which originates from the spatial asymmetry caused by eccentricity. This feature is used for initial fault detection and severity quantification. The second feature is the amplitude of the spectral sidebands, which originates from the temporal modulation produced by a rotating asymmetry. This feature is used to discriminate between SE and DE faults.

2.3. Proposed Method

The first diagnostic feature of the proposed hybrid methodology is the differential phase shift ($\Delta\phi_{diff}$) which quantifies the spatial asymmetry in the stray flux field caused by rotor eccentricity. The analysis uses three flux sensors placed at 120-degree electrical intervals around the machine frame. In a healthy machine, this arrangement produces a set of balanced and predictably phase-shifted signals.

The core principle of this method is to define a baseline signature for the machine under healthy operating conditions served as a zero-reference point. This initial calibration is essential. It compensates for minor inherent machine asymmetries arising from manufacturing tolerances or sensor placement variations. As a result, the diagnostic indicator responds only to anomalies caused by developing faults.

The phase extraction procedure is performed in several steps. First, the time-domain signals from each sensor are transformed into the frequency domain using the Fast Fourier Transform (FFT). From the resulting spectra, the complex value of the fundamental frequency component (f_s) is identified for each signal ($X_A(f_s)$, $X_B(f_s)$ and $X_c(f_s)$). The phase angle of each component is then extracted. The final diagnostic indicator is then calculated. The reference phase differences ($\Delta\phi_{ref,AB}$ and

$\Delta\phi_{ref,AC}$) are initially calculated under healthy conditions using Equation (1).

$$\begin{aligned}\Delta\phi_{ref,AB} &= \angle X_{B,healthy}(f_s) - \angle X_{A,healthy}(f_s) \\ \Delta\phi_{ref,AC} &= \angle X_{C,healthy}(f_s) - \angle X_{A,healthy}(f_s)\end{aligned} \quad (1)$$

These values represent the machine's healthy signature. During online monitoring, the instantaneous phase differences ($\Delta\phi_{meas,AB}$ and $\Delta\phi_{meas,AC}$) are continuously measured, as shown in Equation (2).

$$\begin{aligned}\Delta\phi_{meas,AB} &= \angle X_{B,faulty}(f_s) - \angle X_{A,faulty}(f_s) \\ \Delta\phi_{meas,AC} &= \angle X_{C,faulty}(f_s) - \angle X_{A,faulty}(f_s)\end{aligned} \quad (2)$$

Finally, the differential phase shift is obtained by subtracting the reference values from the measured values as expressed in Equation (3). This differential calculation isolates the phase deviation caused solely by a fault.

$$\begin{aligned}\Delta\phi_{diff,AB} &= \Delta\phi_{meas,AB} - \Delta\phi_{ref,AB} \\ \Delta\phi_{diff,AC} &= \Delta\phi_{meas,AC} - \Delta\phi_{ref,AC}\end{aligned} \quad (3)$$

An eccentricity fault causes a physical distortion in the spatial distribution of the magnetic field. This distortion affects the timing of the flux wave as it reaches each sensor. This effect causes the measured phase differences ($\Delta\phi_{meas}$) to deviate from the healthy reference values ($\Delta\phi_{ref}$). A noticeable non-zero value in the calculated differential phase shift ($\Delta\phi_{diff}$) is therefore a strong indication of an eccentricity fault. Moreover, the magnitude of this phase shift correlates with the severity of the fault. The differential method also offers robustness against common-mode operational variations. Such effects tend to influence all sensor signals in a similar manner. This approach therefore minimizes their impact on the relative phase differences between the sensors.

However, the phase-based analysis cannot reliably distinguish between SE and DE faults. Both fault types produce a similar spatial distortion and therefore a similar phase shift. Consequently, a second feature is required for fault discrimination. This distinction is achieved by analyzing the amplitude of characteristic sideband harmonics in the stray flux spectrum.

A dynamic eccentricity (DE) fault causes a time-varying modulation of the air-gap permeance at the mechanical rotational frequency (f_r). This periodic modulation is the primary source of high-amplitude spectral sidebands. These sidebands appear symmetrically around the fundamental electrical frequency (f_s). The frequencies of these sidebands are determined by the following expressions:

$$f_r = k\frac{f_s}{p} \quad (4)$$

$$f_{pattern} = f_s \pm f_r = (1 \pm k/p) f_s \qquad k = 1, 2, 3, ... \quad (5)$$

In these equations, k is an integer harmonic index and p represents the number of pole pairs. Both SE and DE faults affect the sideband harmonic amplitudes. However, the magnitude of this effect differs significantly between the two fault types. The rotating asymmetry of a DE fault acts as a strong modulation source. This significantly amplifies the sideband amplitudes. The stationary asymmetry of an SE fault is a much weaker modulation source and causes only a slight increase in amplitude.

Therefore, the upper sideband harmonic (USH) at the frequency $f_s(1+1/p)$ is a particularly sensitive indicator for differentiating these faults. The diagnostic logic compares the magnitude of this sideband against a baseline from the healthy condition. This comparison allows for the reliable detection of DE. The method also clearly distinguishes DE from SE. This distinction is possible due to the minimal amplitude response from an SE fault in this frequency region.

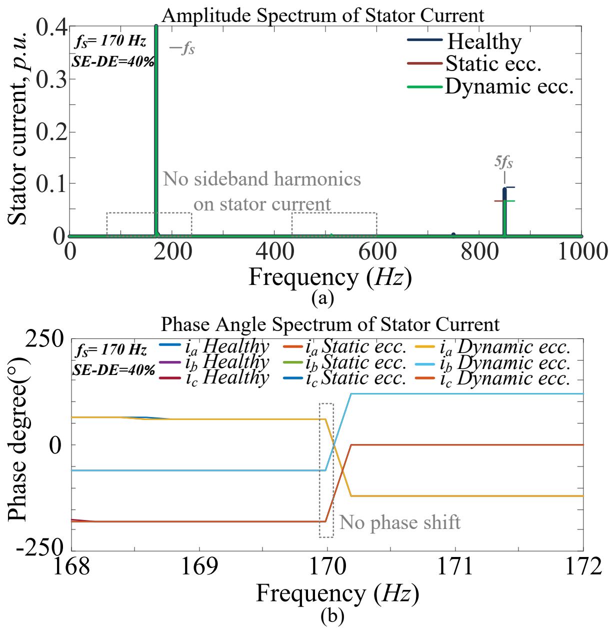

Fig. 2. Spectrums of stator current a) amplitude b) phase angle @40% Static and Dynamic Eccentricity [168-172] Hz

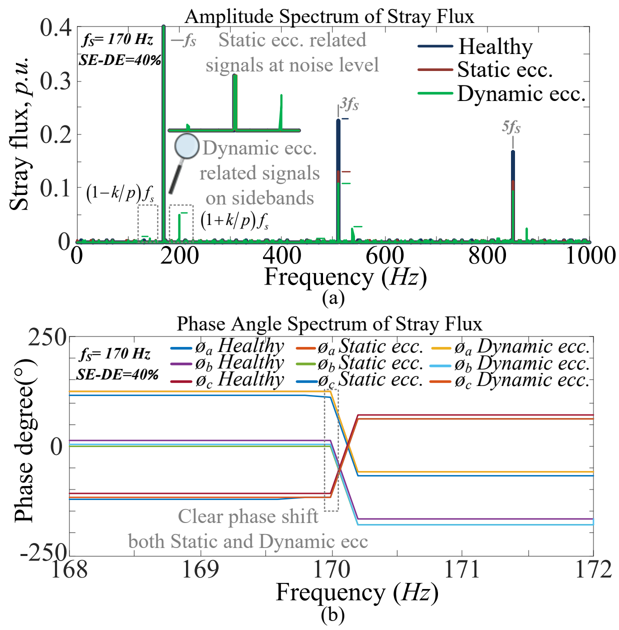

Fig. 3. Spectrums of stray flux a) amplitude b) phase angle @ 40% Static and Dynamic Eccentricity [168-172] Hz

3. Results

This section presents 2D-FEM simulation results for validating the proposed hybrid method. The PMSG model is simulated at 1700 rpm under full load, and data have collected from stator currents and three stray flux sensors under healthy, static (SE) and dynamic eccentricity (DE) conditions. The fault severity has gradually increased from 5% to 60% relative to the nominal air-gap length.

To establish a baseline for comparison, the effects of 40% SE and 40% DE faults on both the stator current and stray flux signal at a single-point have analyzed. The corresponding results are shown in Figure 2 and Figure 3. Figure 2a presents the amplitude spectrum of the stator current. The spectrum shows no significant new components or noticeable changes in sideband amplitudes for either fault type. The spectra for the healthy, SE, and DE cases appear nearly identical. This makes amplitude-based fault detection impractical. Figure 2b presents the phase spectrum of the stator current. This spectrum also fails to provide a faulty signature. No noticeable phase shift is present between the healthy and faulty conditions. Neither amplitude nor phase information provides a clear signature. Therefore, MCSA is unable to detect or differentiate these eccentricity faults under the specified operating conditions.

Analysis of a single-point stray flux signal provides more diagnostic insight compared to the stator current spectrum. Figure 3a presents the amplitude spectrum of this signal. Sideband harmonics appear around the fundamental frequency during fault conditions. These sidebands are significantly more prominent for the DE fault than for the SE fault. This result demonstrates the high sensitivity of stray flux amplitude to dynamic asymmetry. However, the amplitude signature for an SE fault is relatively weak.

Figure 3b presents the phase spectrum and reveals another critical limitation. Both SE and DE faults introduce a significant and nearly identical phase shift. This phase ambiguity prevents reliable fault differentiation with a single sensor. These combined limitations in both amplitude and phase analysis for a single-point measurement highlight the need for a more robust diagnostic strategy. The proposed hybrid analysis approach directly addresses these issues.

The differential phase shift method helps mitigate the influence of certain environmental and operational variations. These can include minor changes in speed and machine temperature. Mitigating these shared operational variations isolates the phase shift caused by magnetic asymmetry and clarifies the resulting fault signature.

Figure 4 illustrates the absolute differential phase shift ($|\Delta\phi_{diff}|$) versus increasing fault severity. The results for both the proposed stray flux analysis (SFA) and MCSA are shown for comparison. These results demonstrate the superior sensitivity of the SFA method. For the SE case, the differential phase shift shows a strong response. It rises sharply from 0° in the healthy state to nearly 20° at only 5% fault severity. As the severity increases to 60%, the phase shift remains high with a slight upward trend. This response is effective for early SE detection and is also suitable for quantifying its severity. The DE fault also produces a significant and stable phase shift. It reaches approximately 18° across all severity levels, confirming the metric's high responsiveness to dynamic eccentricity.

The differential phase shift of the stator current remains near zero under all fault conditions. This result confirms that MCSA is unsuitable for this phase-based analysis. On the other hand, the differential phase shift of the stray flux signal provides a robust indicator for eccentricity. This metric is highly sensitive to the presence of both SE and DE faults. Its magnitude also shows a clear correlation with fault severity, particularly in SE cases. However, the differential phase shift alone is insufficient to differentiate between the two fault types. Therefore, the amplitude of the upper sideband harmonic (USH) is used for fault discrimination.

Figure 5 compares the USH amplitudes for SE and DE faults with severities from 5% to 60%. A substantial amplitude difference exists between the two fault types. At all tested severity levels, the USH amplitude for DE is 170 to 265 times greater than that for SE. This significant difference provides a reliable signature for accurate fault detection.

The combination of phase and amplitude features establishes a systematic diagnostic framework. This framework employs a two-step process of initial detection and subsequent classification. Fault detection is based on the differential phase shift. The fault type is then classified based on the amplitude of the upper sideband harmonic (USH). A low-amplitude USH indicates a static eccentricity (SE) fault. A high-amplitude USH indicates a dynamic eccentricity (DE) fault. The vast difference in amplitude between these two signatures provides the basis for this reliable discrimination.

Proposed hybrid methodology therefore offers a comprehensive diagnosis. Conventional methods often rely on a single metric. This reliance can lead to the diagnostic ambiguities inherent in such approaches. The proposed two-feature approach resolves these ambiguities.

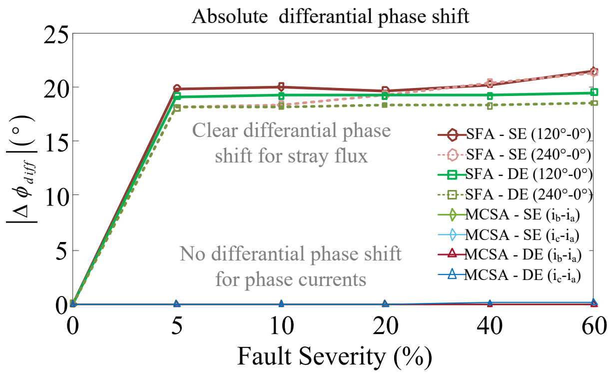

Fig. 4. Absolute differential phase shift versus fault severity for MCSA and SFA

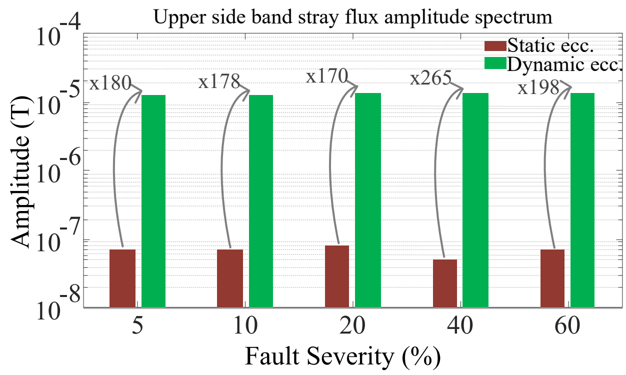

Fig. 5. Comparison of the USH amplitudes of the stray flux signal in SE and DE conditions for different fault severities

4. Conclusions

This study proposed a non-invasive fault detection methodology for eccentricity faults in PMSGs. The methodology is based on the hybrid analysis of phase and amplitude features from the external stray flux signal. This two-feature approach overcomes the diagnostic ambiguities of conventional, single-metric techniques.

The differential phase shift serves as a robust feature for initial fault detection and for quantifying the severity of static eccentricity. The amplitude of the upper sideband harmonic provides the definitive feature for fault discrimination. A dynamic eccentricity fault generates a sideband amplitude 170 to 265 times greater than a static eccentricity fault. This vast disparity in amplitude provides a conclusive basis for fault classification.

The integration of phase and amplitude analysis therefore establishes a comprehensive and reliable diagnostic framework. This framework is demonstrably more reliable than traditional MCSA or single-point stray flux analysis. Future work will focus on the experimental validation of the methodology. Its applicability to mixed eccentricity conditions will also be explored.

5. Acknowledgment

This study was supported by TÜBİTAK (The Scientific and Technological Research Council of Türkiye) under the 2214-A program with Grant No. 1059B142100619

6. References

[1] C. Diao, W. Zhao, Y. Liu, and X. Wang, "Permanent magnet assisted synchronous reluctance motor with asymmetric rotor for high torque performance," *CES Transactions on Electrical Machines and Systems*, vol. 7, no. 2, pp. 179–186, 2023, doi: 10.30941/CESTEMS.2023.00016.

[2] A. Sergakis, M. Salinas, N. Gkiolekas, and K. N. Gyftakis, "A Review of Condition Monitoring of Permanent Magnet Synchronous Machines: Techniques, Challenges and Future Directions," *Energies*, vol. 18, no. 5, p. 1177, 2025, doi: 10.3390/en18031177.

[3] Z. Liu, P. Zhang, S. He, and J. Huang, "A Review of Modeling and Diagnostic Techniques for Eccentricity Fault in Electric Machines," *Energies*, vol. 14, no. 14, p. 4296, 2021, doi: 10.3390/en14144296.

[4] J.-K. Kang and J. Hur, "Fault mechanism analysis of irreversible demagnetization due to the dynamic eccentricity of IPMSM for EV traction," *IEEE Access*, vol. 10, pp. 64483–64494, 2022, doi: 10.1109/ACCESS.2022.3183347.

[5] Y. Qin, G.-J. Li, C. Jia, and P. McKeever, "Investigation of Inter-Turn Short-Circuit Fault of PM Machines Using PWM Voltage-Based Modeling," *IEEE Transactions on Transportation Electrification*, vol. 10, pp. 1324–1334, 2024, doi: 10.1109/TTE.2024.3344457.

[6] B. M. Ebrahimi, J. Faiz, and M. J. Roshtkhari, "Static-, Dynamic-, and Mixed-Eccentricity Fault Diagnoses in Permanent-Magnet Synchronous Motors," *IEEE Transactions on Industrial Electronics*, vol. 56, no. 11, pp. 4727–4739, Nov. 2009, doi: 10.1109/TIE.2009.2029577.

[7] T. Goktas, R. Er, F. Altunel and M. Arkan, "IoT based Multi-Environmental Sensing System: Monitoring of Rotor Fault in Induction Motors," *2023 IEEE 14th International Symposium on Diagnostics for Electrical Machines, Power Electronics and Drives (SDEMPED)*, Chania, Greece, 2023, pp. 285-290, doi: 10.1109/SDEMPED54949.2023.10271411.

[8] M. S. Rafaq, H. Lee, Y. Park, S. B. Lee, D. Fernandez, D. Diaz-Reigosa, and F. Briz, "A Simple Method for Identifying Mass Unbalance Using Vibration Measurement in Permanent Magnet Synchronous Motors," *IEEE Transactions on Industrial Electronics*, vol. 69, no. 6, pp. 6441–6444, 2022, doi: 10.1109/TIE.2021.3088332.

[9] T. Goktas, K. W. Lee, M. Zafarani and B. Akin, "Analysis of magnet defect faults in permanent magnet synchronous motors through fluxgate sensors," *2016 IEEE Applied Power Electronics Conference and Exposition (APEC)*, Long Beach, CA, USA, 2016, pp. 2875-2880, doi: 10.1109/APEC.2016.7468272.

[10]S. Huang, A. Aggarwal, E. G. Strangas, K. Li, F. Niu and X. Huang, "Robust Stator Winding Fault Detection in PMSMs With Respect to Current Controller Bandwidth," *IEEE Transactions on Power Electronics*, vol. 36, no. 5, pp. 5032-5042, May 2021, doi: 10.1109/TPEL.2020.3030036.

[11] Y. Wang, K. Liu, W. Hua, C. Zhang, Z. Wu and H. Zhang, "Analysis and Detection of Rotor Eccentricity in Permanent Magnet Synchronous Machines Based on Linear Hall Sensors," *IEEE Transactions on Power Electronics*, vol. 37, no. 4, pp. 4719-4729, April 2022, doi: 10.1109/TPEL.2021.3131576.

[12] C. Ma, J. Li, N. Zhang, F. Bu, and Z. Yang, "Open-circuit radial stray magnetic flux density based noninvasive diagnosis for mixed eccentricity parameters of interior permanent magnet synchronous motors in electric vehicles," *IEEE Transactions on Industrial Electronics*, vol. 70, no. 2, pp. 1983–1992, 2023, doi: 10.1109/TIE.2022.3165250.

[13] S. R. Mortezaei, M. H. Aliabadi, and S. Javadi, "Eccentricity fault detection in surface-mounted permanent magnet synchronous motors by analytical prediction, FEM evaluation, and experimental magnetic sensing of the stray flux density," *Journal of Magnetism and Magnetic Materials*, vol. 589, p. 171441, 2024, doi: 10.1016/j.jmmm.2023.171441.

[14] Q. Xu, S. Yuan, X. Liu, P. W. T. Pong, and C. Liu, "Online Detection and Location of Eccentricity Fault in PMSG With External Magnetic Sensing," *IEEE Transactions on Industrial Electronics*, vol. 69, no. 10, pp. 9749–9760, Oct. 2022, doi: 10.1109/TIE.2022.3159947.

[15] M. S. Rafaq, *et al*., "Airgap Search Coil Based Identification of PM Synchronous Motor Defects," *IEEE Transactions on Industrial Electronics*, vol. 69, no. 7, pp. 6551–6560, Jul. 2022, doi: 10.1109/TIE.2021.3095810.

[16] K. N. Gyftakis, "Detection of Early Inter-Turn Stator Faults in Induction Motors via Symmetrical Components—Current vs Stray Flux Analysis," in *Proc. IEEE ECCE*, Detroit, MI, USA, 2020, pp. 796–801, doi: 10.1109/ECCE44975.2020.9235689.

[17] I. Aladag, T. Goktas, and M. Arkan, "Discernment of Static Eccentricity and Electrical Load Unbalance Currents through Space Vector Stray Flux in Permanent Magnet Synchronous Generator based Wind Turbines," in *Proc. ELECO 2023*, Bursa, Türkiye, 2023. doi: 10.1109/ELECO60389.2023.10416056